

Details Preserving Multi-Exposure Using Pas Technique

Y. Rakesh¹, Nandam Sai Rupa², Ankam Sangeetha³, Thirumala Balbheem⁴, Masanam Ruchitha⁵
1,2,3,4,5 Department of Electronics and Communication Engineering, PSCMRCE, Vijayawada

ABSTRACT

Due to the development of High Dynamic Range Images, multi-exposure fusion has received a lot of attention in recent years. High dynamic range (HDR) imaging allows for the preservation of natural scenes in the same way that human observers perceive them. Due to the wide dynamic range of natural scenes, significant details in images may be lost when using standard low dynamic range (LDR) capture/display devices. This study proposes an efficient multi-exposure fusion (MEF) approach with a simple yet effective weight extraction method based on principal component analysis, adaptive well-exposedness, and saliency maps to minimise information loss and produce high quality HDRlike images for LDR screens. These weight maps are then refined using a guided filter, and the fusion is performed using a pyramidal decomposition. Experiment results show that the proposed method produces very strong statistical and visual results when compared to existing techniques.

IndexTerms—Image Fusion, PCA, Adaptive Well Exposedness, Saliency Map, Dual Pyramid.

1. INTRODUCTION

Multi-exposure image fusion, in general, refers to the process of combining multiple images with complementary information into a single image with optimal information. High dynamic range (HDR) technology aims to produce high-quality images that are comparable to human perception. By proposing a multi-exposure image fusion scheme, we hope to acquire significant HDR images and improve the subjective and objective evaluation of the fusion effect. MEF's primary goal is to keep the most informative parts of each exposure image by extracting weight maps and then blending them into a single HDRlike image [1]. A weight map extraction scheme based on PCA, adaptive well exposure, and saliency map is proposed. The input stack is fused using the Gaussian pyramid of weight maps and the Laplacian pyramid of exposures. We present a method for more easily incorporating desired image qualities, particularly those relevant for combining different exposures. In this paper, we present a new MEF algorithm that focuses on the design of an efficient and effective weight function. The weight is obtained as a function of pixel values within an image in the set of multi-exposure images in the majority of conventional pixel-wise MEF methods. In other words, existing methods typically apply the same rule to every image in the set, whereas our method employs an adaptive rule across all images. We define three weight functions that may reflect the quality of pixels. The first is to represent the pixel quality in terms of an input image's overall brightness and that of neighbouring exposure images. The weight is intended to be large in the bright areas of the underexposed image and small in the bright areas of the overexposed image. The second weight reflects a pixel's importance when its value is in a range with a relatively large global gradient when compared to other exposure images. The total weight is the sum of these three weights. Because of the simple weight function, the proposed method requires little computational complexity while producing visually appealing results and receiving high scores on an image quality measure. Multi-exposure fusion (MEF) is a popular method for achieving high dynamic range imaging. The selection of features for fusion weight calculation is critical to MEF's performance.

The MEF method generates the weight map by combining three image quality measures (PCA, Adaptive well exposedness, and saliency map) and fusing the images in an efficient multi-resolution framework. A camera's dynamic range is usually less than that of most of the scenes we want to capture. Whatever a camera's bit-depth is, it is considered to have a relatively low dynamic range (LDR) when compared to scenes with a high dynamic range (HDR). As a result, the most common method for capturing such HDR scenes with an LDR camera is to take several pictures while changing the exposure time from short to long [2] and merge to an HDR one.

To display the synthesised HDR image on an LDR display device, however, we need a tone-mapping process to compress the HDR into the LDR [3,4]. When we only have LDR displays as targets, we can directly synthesise a tone-mapped-like LDR image from the multi-exposure images. The multi-exposure image Fusion (MEF) algorithm is commonly used for this purpose. It defines a weight map for each of the multi-exposure images and synthesises a final tone-mapped-like image as a weighted sum of the images. The model incorporates recursive downsampling and processing, and halo effects are significantly reduced. A MEF algorithm based on image linear embeddings and watershed masking is developed in a recent study by Ulucan et al [5]. As a result, the most important task in this approach is determining the appropriate weight maps. Burt et al. [6] used Laplacian pyramid

decomposition to compute weight maps using local efficient energy and pyramid correlation. Mertens et al. [7] defined several pixel quality metrics, including contrast, saturation, and well-exposedness. Raman et al. [8] and Zhang et al. [9] discovered information-rich regions in images using gradient magnitudes or a bilateral filtering process. Because weight maps are frequently noisy, Li et al. [10,11] refined them with edge-preserving filters like the recursive filter or the guided filter [12]. To fuse images, Shen et al. proposed a random walk approach.

PROPOSED METHOD

Flowchart

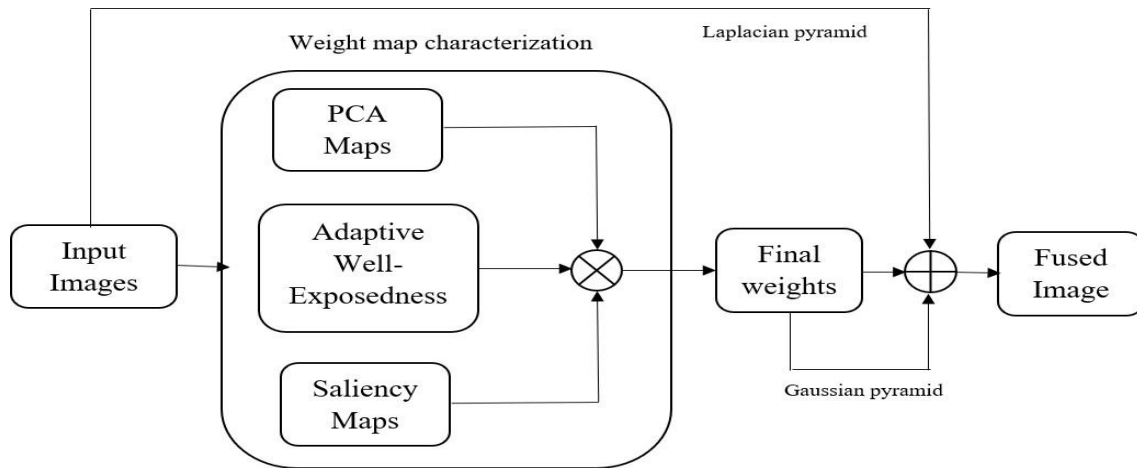


Fig 1 A flowchart of the proposed method

We have three types of maps for input exposures. Adaptive well exposure, PCA, and Saliency map We get a final weight by combining these three techniques in order to output a fused image via pyramidal decomposition.

PCA Weight Extraction Technique

A linear dimensionality reduction technique that converts a set of correlated elements into a smaller number of uncorrelated elements. It is used to reduce the dimensionality of large data sets by transforming a large set of variables into a smaller one that retains the majority of the information from the larger set. When performing PCA on images, one must create a flat vector of features, where each pixel's intensity is a feature and each image is represented as a flat vector. For example, if you have 16x16 grayscale images, you should convert them to 256 values and use PCA on that data; it is one of the most well-known data compression techniques [13]

PCA assists us in identifying patterns based on their correlation, or it is simply a feature extraction technique that allows us to drop the least important information while retaining the important information in the dataset.

How does PCA reduce the number of image dimensions?

Majorly four steps

- (1) Normalize image data
- (2) Calculate covariance matrix from image data
- (3) Perform single value decomposition
- (4) Find projection of image data on the basis of reduced features.

PCA uses an orthogonal transformation to produce linearly uncorrelated variables from potentially correlated data [14]. Using the eigenvectors of the covariance matrix, the correlated data is projected onto the PCA space. The first principal component is in the direction of the greatest variance (first eigenvector), while the second is in the subspace perpendicular to the first, and the subsequent principal components are computed in the same manner. Data representations in the PCA space are known as scores.

PCA has already been used in image fusion but, to the best of available knowledge, it has not been employed in MEF studies [14]. Therefore, it is investigated in this study first by vectorizing N number of gray-scale versions of exposure images $I_n, n= 1...N$, into column vectors of the size $rc \times 1$ where r and c represent the number of rows and columns of each image, respectively. The obtained N column vectors are then stacked into the columns of an $rc \times$

N data matrix, in which there are r observations with N variables each, for calculating the scores of observations via PCA. Subsequently, each variable-score vector is linearly normalised to have a range of [0 1], then reshaped to a rc matrix and smoothed with a simple smoothing Gaussian filter. Finally, N PCA weight maps (P_n) are generated using a sum-to-one normalisation at each spatial position.

Adaptive Well Exposedness Weight extraction Technique

Adaptive well exposure is a feature used in weight extraction. It will extract each red-green-blue channel separately for a given exposure image using the Gaussian Curve as the extraction method.

$$e^{(x_n - 0.5)^2 / 2\sigma^2}$$

where, $\sigma = 0.2$

The weight aims to maintain pixel intensities that are not close to 0 or 1. As a result, the favour pixel intensity in well-exposed pixels for weight extraction will be close to 0.5. However, the well-exposedness feature is not always sufficient for preserving bright-exposure images [15]. To address this issue, we proposed well-exposure based on the mean of pixel intensities in the exposure image. We changed the contrast value to 0.5 and replaced it with some functions of the mean of the pixel intensities of x_n and its neighbouring exposure images, x_{n-1} and x_{n+1} . So, the adaptive well exposedness that we proposed is used to allocate large weights to dark regions when the image is long exposed and small weights to bright regions when the image is short exposed [15]. All computations are performed on the luminance channel Z_n of X_n , as specified in eq (1)

$$E_n = e^{\frac{x_n - (1 - 2\mu x_n)^2}{2\sigma x_n}} \text{-----(1)}$$

Where σX_n and μX_n represent the mean and standard deviation of pixel intensities, respectively. Finally, it provides an adaptive algorithm because Gaussian curve controlling parameters are extracted from statistical data of each individual exposure and large weights are assigned to the best luminance intensities of the input. we can depict the obtained adaptive well-exposedness weight E_n of the Ulucan stack.

Saliency Map Weight extraction technique:

A saliency map is simply a region in an image that is highlighted and first noticed by the human eye. This saliency map can be used to extract weight. The absolute value of the difference between the intensity of the pixel and the reference grayscale intensity is determined for this purpose. Saliency maps are used in this process to assign higher weights to image regions that are more appealing to the human eye. This technique, developed by Hou et al [16], is implemented in the proposed MEF method. This has a specific algorithm known as the saliency algorithm. It is a method of determining the most relevant in an image while spending less time and energy. It uses machine learning to extract information about important, relevant data from any given image by locating salient regions and points, and it is based on image signature. The image signature is the sign of the Discrete Cosine Transform (DCT) coefficients. Finally, the saliency maps are derived from the reconstructed image. The reader can find more information about this in [16].

Final weight and Fusion

After characterizing all three weight maps, they are combined to form a single refined map for each exposure in the input stack given in eq (2) as follows

$$w_n = Guidfilt(P_n * X_n * S_n) \text{-----(2)}$$

$$n = 1, 2, \dots, m$$

Where Guidfilt is an edge-preserving (smoothing) filter, it is referred to as a guided filter [17]. This guided filter is applied to weight maps to reduce discontinuities and noise. To form the final weight for fusion, all of these weight maps are normalized to satisfy a sum to one at spatial positions.

Pyramidal decomposition is used to avoid artifacts such as the halo effect at sharp texture and colour transitions. In particular, the laplacian pyramid is used to decompose each input exposure level of distinct resolution, whereas the Gaussian pyramid is used to perform the same operation for final fusion weights. This operation is performed at each pyramid level, yielding a fused laplacian pyramid for the fused image given in eq(3)

$$L\{F^l\} = \sum_{n=1} G\{w^l\} * L\{I^l\} \text{-----}(3)$$

where the fused pyramid $L\{F^l\}$ is eventually collapsed to obtain the final fused image F .

The weight map extraction algorithm relies on principal component analysis (PCA), adaptive well-exposedness and saliency map features. These maps are later refined by a guided filter, and then exposure images are fused via a pyramidal decomposition. The proposed method is compared with well-known MEF algorithms and it demonstrates very strong outputs both statistically and visually.

3. Experimental results

The proposed MEF algorithm (MEF-PAS) is compared to Mertens [1], Ulucan [2]. MATLAB R2019b is used to run all experiments on an AMD Ryzen(TM)3 3200x CPU @ 3.5 GHz 2-core 4GB RAM machine. All competing algorithms, including the proposed method, are used with their default settings with no optimization. The MEF-SSIM multi-scale structural similarity framework [18] is used to conduct a statistical performance analysis. MEF-SSIM is a perceptual quality assessment metric that produces statistical results in the [0 1] range by taking into account both global luminance consistency and local structure preservation. A higher score reflects higher perceptual quality.

Table 1 shows the statistical scores obtained for all algorithms. We calculated runtime, MEF SSIM, and MSE (mean square error of our method). For this exposure sequence, MEF-PAS yields the highest MEF-SSIM score. When compared to mertens1 and ulcan5, which have lower brightness and less information in several parts of the fused image, the proposed method clearly preserves the details of the Flower, Belgium, and Venice. The walls in Ulucan, on the other hand, have a more plausible colour.

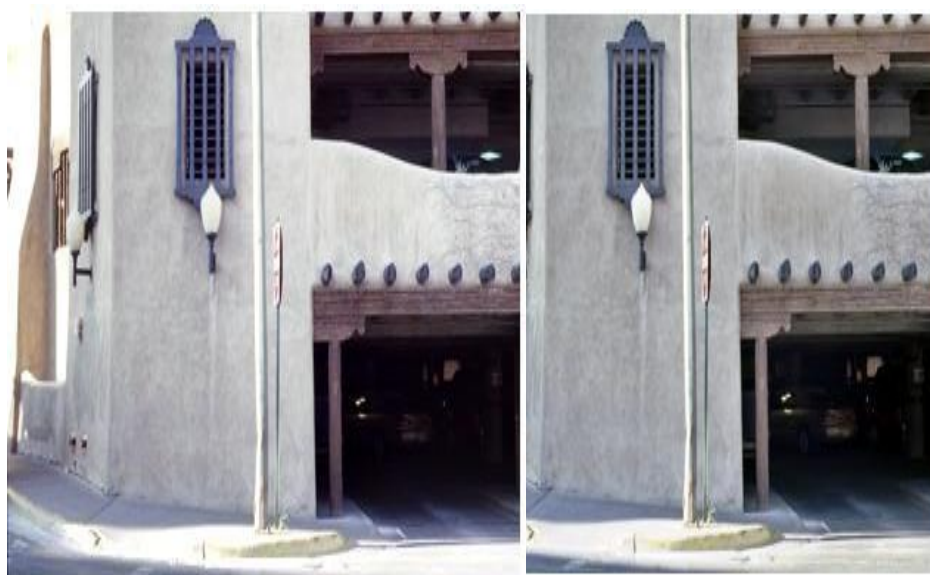


Fig 2 Building Ulucan (Left), Ours (Right)

Figure 2 depicts a visual comparison of the building stack fusion outputs from PASMEF and Ulucan. In this example, PAS-MEF achieves the highest MEF-SSIM score when compared to other competing techniques. The PASMEF output clearly shows that the colour of the building is more natural. Figure 3 depicts a further visual comparison for Belgium. The proposed PAS-MEF recovers light and building colour much better, preserving trees and ensuring that Belgium has vibrant colours in Ulucan.



Fig 3 Belgium Ulucan (Left), Ours (Right)

The fusion outputs of MEF-PAS for the Ulucan stack are compared in Fig. 4. Although PAS-MEF has the lowest MEFSSIM score of any stack in the dataset for this exposure sequence, the background has more well-settled colours in light regions, and the chairs and walls have more vivid colours when compared to Ulucan, whose MEFSSIM is slightly higher.

Weight maps are first defined using linear embeddings of exposure image patch spaces while preserving the sampled manifold structure's local geometry. Watershed masking is then used to refine these weight maps to highlight the most informative parts of each exposure in the input stack. Finally, the fusion process is carried out using weighted averaging. More fusion examples are shown in Figs. 3 and 4 for Building and Belgium, respectively. PAS-MEF produces more vibrant colours for the building, doors, and trees in the background, whereas Ulucan produces a darker output[5].

	MEF-SSIM	Run time	MEF-SSIM	Run time	MEF-SSIM	Run time	Mean square error
Building	0.925	1.8459	0.9337	13.0503	0.921	0.3052	0.1048
Belgium house	0.962	1.3776	0.9641	16.4578	0.968	0.5308	2.7592
Chairs	0.938	1.4898	0.9454	12.7819	0.949	0.3721	5.4595
Church	0.972	1.8005	0.9732	12.8199	0.973	0.3464	5.2449
House	0.919	1.5519	0.8984	12.6676	0.936	0.2773	2.0707
Venice	0.954	1.5845	0.9424	15.5977	0.978	0.3037	3.5824
Demo-IzmirNight	0.985	1.6252	0.9927	31.4614	0.98	1.3033	4.9393
Flower	0.938	1.8102	0.9467	6.024	0.963	0.2946	5.7874

Table 1: MEF-SSIM scores for each exposure stack used in experiments.

As it can be deduced from above studies, each specific algorithm generally differs in the way of extraction and/or characterization of weight maps. Therefore, new weight map extraction methods will enlighten the path leading to a general map formation framework. To this end, in this paper, a novel MEF method is proposed to fuse static exposure stacks. The weight map extraction algorithm relies on principal component analysis (PCA), adaptive well-exposedness and saliency map feature



Fig 4 Chairs Ulucan (Left), Ours (Right)

In Fig. 5, the fusion results are presented for the *Mask* stack. PAS-MEF produces the highest MEF-SSIM score (together with Hayat) for this exposure sequence. When compared to Ulucan [5] which has lower brightness and less information in several parts in the fused image, the proposed method clearly preserves the details of the building and the Venice, and Flowers are clearer when compared to Ulucan [5]. In Fig. 5, the fusion outputs of PAS-MEF and Mertens are compared for the *Ulucan* stack. Although PAS-MEF has its lowest MEFSSIM score for this exposure sequence among other stacks in the dataset, the sky has more well-settled colors in blue regions, and the rooftop of the house and the grass have more vivid colors when compared to Hayat, whose MEF-SSIM is slightly higher. The fusion outputs of PAS-MEF and Hayat are compared for the *Ulucan* stack. Although PAS-MEF has its lowest MEFSSIM score for this exposure sequence among other stacks in the dataset, the lighting has more well-settled colors in bright regions, and the rooftop of the house and the walls have more vivid colors when compared to Ulucan and Mertens, whose MEF-SSIM is slightly higher. The building has more well-settled colors in PAS-MEF which has the highest MEF-SSIM score when compared to other methods. The proposed method is compared with well-known MEF algorithms and it demonstrates very strong outputs both statistically and visually. These weight maps are then refined via watershed masking to highlight most informative parts of each exposure in the input stack. Exposure sequence among other stacks in the dataset, the sky has more well-settled colors in blue regions, and the rooftop of the house and the grass have more vivid colors when compared to Hayat, whose MEF-SSIM is slightly higher. The building has more well-settled colors in PAS-MEF which has the highest MEF-SSIM score when compared to other methods.



Fig 5 church: Ulucan (Left), Ours (Right)

The proposed method is compared with well-known MEF algorithms and it demonstrates very strong outputs both statistically and visually. These weight maps are then refined via watershed masking to highlight most informative parts of each exposure in the input stack. Exposure sequence among other stacks in the dataset, the sky has more well-settled colors in blue regions, and the rooftop of the house and the grass have more vivid colors when compared to Hayat, whose MEF-SSIM is slightly higher.



Fig 6 House Ulucan (Left), Ours (Right)

Further fusion examples are illustrated in Fig. 4 and Fig. 6 for *Chairs* and *House*, respectively. The rooftop of the Church, books and Chairs in the background have more striking colors in PAS-MEF, while a darker output is generated by Ulucan. Next in Fig. 5, Ulucan contains very bright regions on the house. The house has more well-settled colors in PAS-MEF which has the highest MEF-SSIM score when compared to other methods. Weights maps are first characterized via linear embeddings of exposure image patch spaces, while preserving local geometry of the sampled manifold structure.

CONCLUSION

The proposed MEF is widely used for obtaining HDR-like high quality images, and numerous studies in this field are available. In general, the weight map characterization process differs between existing methods. The weight extraction method based on PCA, adaptive well-exposedness, and saliency map is introduced in this paper. The obtained weights are refined using a guided filter, and image fusion is performed using pyramidal decomposition. Both statistically and practically, the proposed algorithm produces very strong results.

In the future, the proposed algorithm will be optimised to improve its statistical and virtual performances while also reducing run-time complexity.

REFERENCES

- [1] T. Mertens, J. Kautz, and F. Van Reeth, "Exposure fusion: a simple and practical alternative to high dynamic range photography," *Comp. Graph. Forum*, vol. 28, no. 1, pp. 161–171, February 2009.
- [2] Paul E Debevec and Jitendra Malik, "Recovering high dynamic range radiance maps from photographs," in *Proceedings of the 24th annual conference on Computer graphics and interactive techniques*. ACM Press/Addison-Wesley Publishing Co., 1997, pp. 369–378.
- [3] Fredo Durand and Julie Dorsey, "Fast bilateral filtering for the display of high-dynamic-range images," in *ACM transactions on graphics (TOG)*. ACM, 2002, vol. 21, pp. 257–266.
- [4] Erik Reinhard, Michael Stark, Peter Shirley, and James Ferwerda, "Photographic tone reproduction for digital images," *ACM transactions on graphics (TOG)*, vol. 21, no. 3, pp. 267–276, 2002.
- [5] O. Ulucan, D. Karakaya, and M. Turkan, "Multi-exposure image fusion based on linear embeddings and watershed masking," *Signal Process.*, vol. 178, pp. 107791, January 2021.
- [6] Peter J Burt and Raymond J Kolczynski, "Enhanced image capture through fusion," in *Computer Vision, 1993. Proceedings., Fourth International Conference on*. IEEE, 1993, pp. 173–182.
- [7] Tom Mertens, Jan Kautz, and Frank Van Reeth, "Exposure fusion: A simple and practical alternative to high dynamic range photography," in *Computer Graphics Forum*. Wiley Online Library, 2009, vol. 28, pp. 161–171.
- [8] Shanmuganathan Raman and Subhasis Chaudhuri, "Bilateral filter-based compositing for variable exposure

- photography,” in Eurographics (Short Papers), 2009, pp. 1–4.
- [9] Wei Zhang and Wai-Kuen Cham, “Gradient-directed multiexposure composition,” *IEEE Transactions on Image Processing*, vol. 21, no. 4, pp. 2318–2323, 2012.
- [10] Shutao Li, Xudong Kang, and Jianwen Hu, “Image fusion with guided filtering,” *IEEE Transactions on Image Processing*, vol. 22, no. 7, pp. 2864–2875, 2013.
- [11] Eduardo SL Gastal and Manuel M Oliveira, “Domain transform for edge-aware image and video processing,” in *ACM Transactions on Graphics (ToG)*. ACM, 2011, vol. 30, p. 69.
- [12] Kaiming He, Jian Sun, and Xiaoou Tang, “Guided image filtering,” in *European conference on computer vision*. Springer, 2010, pp. 1–14.
- [13] S. Wold, K. Esbensen, and P. Geladi, “Principal component analysis,” *Chemom. Intell. Lab. Syst.*, vol.2, no. 1-3, pp. 37-52, August 1987.
- [14] S. Li, X. Kang, L. Fang, J. Hu, and H. Yin, “Pixel-level image fusion: A survey of the state of the art,” *Inf. Fusion*, vol. 33, pp. 100–112, January 2017.
- [15] X.Hou, J.Harel, and C.Koch, “Image signature: Highlighting sparse salient regions,” *IEEE Trans. Pattern Anal. Mach. Intell.*, vol. 34, no.1, pp. 194-201, January 2012.
- [16] S. Lee, J.S.Park, and N.I.Cho, “A multi-exposure image fusion based on the adaptive weights reflecting the relative pixel intensity and global gradient,” in *IEEE Int. Conf. Image Process.*, 2018, pp.1737-1741.
- [17] K. He, J. Sun, and X. Tang, “Guided image filtering,” in *Eur. Conf. Comput. Vision*, 2010, pp.1-14.
- [18] K. Ma, K. Zeng, and Z. Wang, “Perceptual quality assessment for multi-exposure image fusion,” *IEEE Trans. Image Process.*, vol. 24, no. 11, pp. 3345–3356, June 2015.
- [19] Kranthi Kumar, S., Ramana, K., Dhiman, G., Singh, S., & Yoon, B. (2021). A Novel Blockchain and Bi-Linear Polynomial-Based QCP-ABE Framework for Privacy and Security over the Complex Cloud Data. *Sensors*, 21(21), 7300.
- [20] Singamaneni, Kranthi Kumar, Pasala Sanyasi Naidu, and Pasupuleti Venkata Siva Kumar. "Efficient quantum cryptography technique for key distribution Efficient quantum cryptography technique for key distribution."
- [21] Singamaneni, Kranthi Kumar, and Pasala Naidu. "Secure key management in cloud environment using quantum cryptography." *Ingénierie des Systèmes d'Information* 23.5 (2018).
- [22] Singamaneni, Kranthi Kumar, and Pasala Sanyasi Naidu. "IBLIND Quantum Computing and HASBE for Secure Cloud Data Storage and Accessing." *Rev. d'Intelligence Artif.* 33.1 (2019): 33-37.
- [23] Singamaneni, Kranthi Kumar, Pasala Sanyasi Naidu, and Pasupuleti Venkata Siva Kumar. "Efficient quantum cryptography technique for key distribution." *Journal Europeen des Systemes Automatises* 51.4-6 (2018): 283.
- [24] Singamaneni, Kranthi, Abdullah Shawan Alotaibi, and Purnendu Shekhar Pandey. "The Performance Analysis and Security Aspects of Manet." *ECS Transactions* 107.1 (2022): 10945.
- [25] S. Kranthi Kumar, A. Alolo Abdul-Rasheed Akeji, T. Mithun, M. Ambika, L. Jabasheela et al., "Stock price prediction using optimal network based twitter sentiment analysis," *Intelligent Automation & Soft Computing*, vol. 33, no.2, pp. 1217–1227, 2022.
- [26] Rekha Baghel, D.Saravanan, et.al., “Reclamation of extraordinary utility items in the multi-level catalogue”, *Recent Trends in Science and Engineering*, AIP Conf. Proc. 2393, 020195-1–020195-11; <https://doi.org/10.1063/5.0074502>, Published by AIP Publishing. 978-0-7354-4198-9/\$30.00.
- [27] D.Saravanan, et.al., “Optimization of Machine Learning and Deep Learning Algorithms for Diagnosis of Cancer”, *ECS Transactions*, Volume 107, Number 1, DOI: <https://doi.org/10.1149/10701.9389ecst>.
- [28] D.Saravanan, et.al., “Customer Relationship Management in Banking in the UK Industry: Case of Lloyds Bank”, *ECS Transactions*, Volume 107, Number 1, DOI: <https://doi.org/10.1149/10701.14325ecst>.
- [29] D.Saravanan, et.al., ”Brand Influencing Customers Buying Behaviors: A Case Study on Nike”, *ECS Transactions*, Volume 107, Number 1, DOI: <https://doi.org/10.1149/10701.5597ecst>.
- [30] D.Saravanan, et.al., “Simulation of Carbon Nanotubes and NANO Based Material for Molecular Device Applications”, *ECS Transactions*, Volume 107, Number 1, DOI: <https://doi.org/10.1149/10701.13403ecst>.
- [31] D.Saravanan, et.al., “Customer Relationship Management in Banking in the UK Industry: Case of Lloyds Bank”, *ECS Transactions*, Volume 107, Number 1, DOI: <https://doi.org/10.1149/10701.14325ecst>.
- [32] D Saravanan, K Santhosh Kumar, “IoT based improved air quality index prediction using hybrid FA-ANN-ARMA model”, *Elsevier Materials Today Proceedings*.
- [33] DL Shanthi, K Arumugam, D. Saravanan, et.al., “Optimized artificial neural network assisted trade-off between transmission and delay in LTE networks”, *Elsevier Materials Today Proceedings*.

- [34] M Chandragowda, D Saravanan, et.al., "Consequence of silane combination representative on the mechanical possessions of sugarcane bagasse and polypropylene amalgams", Elsevier Materials Today Proceedings.
- [35] A Srinivasa Rao, D Saravanan, et.al., "Supervision calamity of public opinion actions based on field programmable gate array and machine learning", International Journal of Nonlinear Analysis and Applications, Volume No:12, Issue No:2, July 2021.
- [36] R. Abish, D. Stalin David, "Detecting Packet Drop Attacks in Wireless Sensor Networks using Bloom Filter", International Journal of Scientific Research in Computer Science, Engineering and Information Technology (IJSRCSEIT), ISSN : 2456-3307, Volume 2 Issue 2, pp. 730-735, March-April 2017.
- [37] A. Vignesh, D. Stalin David, "Novel based Intelligent Parking System", International Journal of Scientific Research in Computer Science, Engineering and Information Technology (IJSRCSEIT), ISSN : 2456-3307, Volume 2 Issue 2, pp. 724-729, March-April 2017.
- [38] D Stalin David, 2020, „Diagnosis of Alzheimer's Disease Using Principal Component Analysis and Support Vector Machine, International Journal of Pharmaceutical Research, Volume 12, Issue 2, PP.713-724.
- [39] Jaswanth K S, Dr. D. Stalin David, "A Novel Based 3d Facial Expression Detection Using Recurrent Neural Network", International Journal of Scientific Research in Computer Science, Engineering and Information Technology (IJSRCSEIT), ISSN : 2456-3307, Volume 6 Issue 2, pp. 48-53, March-April 2020.
- [40] D Stalin David, 2020, „An Intellectual Individual Performance Abnormality Discovery System in Civic Surroundings“ International Journal of Innovative Technology and Exploring Engineering, Volume 9, Issue 5, PP.2196-2206.
- [41] D Stalin David, 2020, „Machine learning for the prelude diagnosis of dementia“, International Journal of Pharmaceutical Research, Volume 13, Issue 3, PP.2329-2335.
- [42] David, D.S. and Y. Justin, 2020. A Comprehensive Review on Partition of the Blood Vessel and Optic Discin Retinal Images. Artech J. Eff. Res. Eng. Technol., 1: 110-117.
- [43] Stalin David D, Saravanan M, "Enhanced Glaucoma Detection Using Ensemble based CNN and Spatially Based Ellipse Fitting Curve Model", Solid State Technology, Volume 63, Issue 6, PP.3581-3598.
- [44] Stalin David D, Saravanan M, Jayachandran A, "Deep Convolutional Neural Network based Early Diagnosis of multi class brain tumour classification", Solid State Technology, Volume 63, Issue 6, PP.3599- 3623.
- [45] Dr. D. Stalin David, Mr. D. Saravanan, "Certain Investigation On Iot Therapeutic Image Recognition And Rivaroxabanpreclude Thrombosis In Patients", 2021, pg.no:51-66, ISBN: 978-81-948555-1-4.
- [46] R.Parthiban, Dr.K.Santhosh Kumar, Dr.R.Sathya, D.Saravanan," A Secure Data Transmission And Effective Heart Disease Monitoring Scheme Using Mecc And Dlmnn In The Cloud With The Help Of Iot", International Journal of Grid and Distributed Computing, ISSN: 2005 – 4262, Vol. 13, No. 2, (2020), pp. 834 – 856.
- [47] R.Bhavya, G.I.Archanaa, D.Karthika, D.Saravanan," Reflex Recognition of Tb Via Shade Duplicate Separation Built on Geometric Routine", International Journal of Pure and Applied Mathematics 119 (14), 831- 836.
- [48] D Saravanan, R Bhavya, GI Archanaa, D Karthika, R Subban," Research on Detection of Mycobacterium Tuberculosis from Microscopic Sputum Smear Images Using Image Segmentation", 2017 IEEE International Conference on Computational Intelligence and Computing Research (ICCIC).
- [49] D Saravanan, R Parthiban," Automatic Detection of Tuberculosis Using Color Image Segmentation and Statistical Methods", International Journal of Advance Research in Science and Engineering, Volume 6, Issue 10.
- [50] U.Palani, D.Saravanan, R.Parthiban, S.Usharani," Lossy Node Elimination Based on Link Stability Algorithm in Wireless Sensor Network", International Journal of Recent Technology and Engineering (IJRTE), Volume 7, Issue 6S5.
- [51] S.G.Sandhya, D.Saravanan, U.Palani, S.Usharani," Handover Priority to the Data at Knob Level in Vanet", International Journal of Recent Technology and Engineering (IJRTE), Volume 7, Issue 6S5.
- [52] D.Saravanan R.Parthiban, U.Palani S.G.Sandhya," Sheltered and Efficient Statistics Discrimination for Cluster Based Wireless Antenna Networks", International Journal of Recent Technology and Engineering (IJRTE), Volume 7, Issue 6S5.
- [53] Raghu Raman D, Saravanan D, Nivedha R," An Efficacious E-Portal for Rancher to BuySeeds and Humus", International Journal of Recent Technology and Engineering (IJRTE), Volume-8, Issue-1S5, June 2019.